Interface Shear Damage to a HDPE Geomembrane. II: Gravel Drainage Layer

Patrick J. Fox, M.ASCE[1]; and Stuart S. Thielmann[2]

Abstract: An experimental program of large-scale direct shear tests has indicated that shear displacement of a gravel drainage layer and nonwoven geotextile protection layer over a high-density polyethylene (HDPE) geomembrane under moderate to high normal stress conditions can cause much greater damage to the geomembrane than static pressure alone. Essentially, no damage was observed at low normal stress. The greatest damage occurred at high normal stress (1,389 kPa) using a lightweight geotextile ($335\ \mathrm{g/m^2}$) and yielded an average of $31\ \mathrm{holes/m^2}$, with a maximum hole size of 29 mm. Surprisingly, geomembrane damage measured using a lightweight geotextile was greater than that measured using no geotextile due to a change in failure surface location. For the same conditions, shear-induced damage was slightly less for a geomembrane placed on a compacted sand subgrade than on a compacted clay subgrade. Interface shear strength increased significantly with decreasing geotextile mass/area due to greater out-of-plane deformation of the geomembrane. The findings suggest that the placement of a gravel drainage layer on top of a HDPE geomembrane, even with a protection nonwoven geotextile, should be viewed with caution for landfill bottom liner systems and other moderate- to high-stress applications. If there is a reasonable expectation for interface shear displacement, project-specific direct shear tests should be conducted to determine the potential for shear-induced geomembrane damage. Recommendations are provided for the performance of such tests and for design options when damage mitigation is necessary. **DOI: 10.1061/(ASCE)GT.1943-5606.0001120.**

Author keywords: Geomembrane (GM); Geotextile (GT); Gravel; Drainage layer; Interface shear; Direct shear; Damage.

Introduction

Geomembranes (GMs) are commonly used in composite liners for landfills and other engineered facilities, and are generally considered to be excellent hydraulic barriers provided that physical damage in the form of tears and punctures is minimized. The greatest risk of damage to a geomembrane is associated with stress concentrations from contact with coarse soil particles (e.g., gravel and stones), which can occur from an underlying soil subgrade or an overlying granular soil layer (Nosko and Touze-Foltz 2000; Giroud and Touze-Foltz 2003). Accordingly, protection layers are used to guard against puncture from such particles and limit associated tensile strains that may lead to the development of holes in a geomembrane over time (Rowe et al. 2004; Peggs et al. 2005).

Since the first proposed usage of geotextiles (GTs) as cushions for geomembranes (Giroud 1973, 1982), extensive research has been conducted on the development and assessment of geomembrane protection layers. Although some studies have investigated damage that occurs during construction operations (Heerten 1994; Reddy et al. 1996a), most of this work has focused on damage due to static overburden pressure. These investigations have led to the development of materials, test methods, design guidelines, and standards of practice to protect geomembranes from static pressure damage. For example, a wide variety of materials, including geotextiles, geonets, geocomposites, geosynthetic clay liners (GCLs), tire shreds, clay, sand, and sand-filled cushions, have been investigated for their ability to provide geomembrane protection, with nonwoven (NW) geotextiles now being the preferred choice for most designs. Likewise, various kinds of static pressure tests have been conducted for these assessments (Hullings and Koerner 1991; Motan et al. 1993; Narejo et al. 1996; Zanzinger 1999; Tognon et al. 2000; Dickinson and Brachman 2008; Koerner et al. 2010; Hornsey and Wishaw 2012; Brachman and Sabir 2013). The resulting standard of practice for landfill composite liners in the United States is to place a GM on a GCL or smooth compacted clay liner (CCL) and then cover the geomembrane with a NW GT for protection. For bottom liner systems, the nonwoven geotextile typically has a mass per unit area of $335-540\ \mathrm{g/m^2}$ and is rarely as heavy as $810\ \mathrm{g/m^2}$. The foregoing body of research, which has led to this and other similar standards of practice, has however not accounted for possible additional geomembrane damage that can occur when static pressure is combined with interface shear.

Interface shear displacements can occur within liner systems due to a variety of mechanisms, including waste settlement, seismic loading, and stress transfer from nearby slopes (Stark and Poeppel 1994; Reddy et al. 1996b; Filz et al. 2001; Jones and Dixon 2005; Zania et al. 2010; Kavazanjian et al. 2011). Depending on conditions, these displacements can be large. For example, numerical simulations have indicated that waste settlement can produce shear displacements exceeding 1 m on the side slopes of a bottom liner system, even for a globally stable design (Dixon et al. 2012; Sia and Dixon 2012). A large-scale field test has also measured significant shear displacements, going into the postpeak range, for a NW GT/GM interface on a side slope due to veneer sand and early waste loading (Zamara et al. 2012). Such displacements are particularly likely for geomembrane interfaces because shear strengths with adjacent materials (e.g., CCLs and NW GTs) are often critical for stability analysis. Assessment of geomembrane integrity for interface shear

[1]Professor, Dept. of Structural Engineering, Univ. of California–San Diego, La Jolla, CA 92093 (corresponding author). E-mail: pjfox@ucsd.edu

[2]Development Engineer, Dept. of Structural Engineering, Univ. of California–San Diego, La Jolla, CA 92093.

Note. This manuscript was submitted on April 15, 2013; approved on February 20, 2014; published online on April 28, 2014. Discussion period open until September 28, 2014; separate discussions must be submitted for individual papers. This paper is part of the ***Journal of Geotechnical and Geoenvironmental Engineering***, © ASCE, ISSN 1090-0241/04014040(12)/$25.00.

conditions is therefore warranted, especially considering that local movements are buried within a landfill and any resulting damage is unlikely to be detected and repaired.

The potential for geomembrane damage from interface shear against coarse particles has only recently been studied for gravelly subgrade soils. Fox et al. (2011) evaluated the integrity of linear low-density polyethylene (LLDPE) and high-density polyethylene (HDPE) geomembranes under specific operational conditions for a mineral reclamation facility and found that interface shear over gravelly sand can produce greater geomembrane damage than static pressure alone. In the companion paper, Fox et al. (2014) conducted a broader investigation of HDPE geomembranes sheared over gravelly CCLs for varying conditions of normal stress, CCL gravel content, CCL water content, and interface shear displacement. In each case, geomembrane integrity was assessed after sustained static pressure (i.e., prior to shear) and after shear to large displacement. The results indicate that HDPE geomembranes can be seriously damaged from interface shear over a gravelly CCL at moderate to high normal stress levels and that such damage can be greatly reduced by placement of a needle-punched GCL at the GM/CCL interface. Results from the Fox et al. (2014) investigation suggest that shear-induced damage may be an important consideration for geomembranes that interface with other coarse soils, such as an overlying granular drainage layer (DL), under moderate to high normal stress conditions. This case is particularly relevant for landfill bottom liners because long-term leachate permeation tests have consistently indicated that clogging of a leachate collection system can be expected to decrease with increasing particle size and that coarse gravel performs better than finer grained materials (Rowe et al. 2000; Fleming and Rowe 2004; McIsaac and Rowe 2007). Heap leach pads represent another application in which geomembranes are often placed in contact with soils containing gravel and under high normal stress (Thiel and Smith 2003; Christie and Smith 2013).

This paper is the second of a companion pair of papers that present the findings of an experimental investigation of damage to HDPE geomembranes when placed against coarse (i.e., gravelly) soils and subjected to static pressure and large displacement interface shear. The focus of this paper is geomembrane damage that results from interface shear with an overlying gravel drainage layer. Fox and Thielmann (2014) discussed some of the findings. Large-scale direct shear tests were conducted using two subgrade soils, three normal stress levels, and three nonwoven geotextiles for geomembrane protection. In each case, geomembrane integrity was assessed after sustained static pressure and after interface shear to large displacement. Implications of the findings with regard to engineering practice are discussed and future research needs are identified for applications in which a gravel drainage layer is placed over a geomembrane, with and without a protection nonwoven geotextile at the interface.

Experimental Program

Materials

The experimental program was conducted using two common geosynthetic products. The HDPE geomembrane was manufactured by Poly-Flex, Inc. (Grand Prairie, Texas). Geomembrane specimens had a thickness of 1.5 mm, blown-film texturing on both sides, and the material properties given in Table 1. Three polypropylene staple fiber nonwoven geotextiles, manufactured by GSE Lining Technology (Houston, Texas), were used as protection layers. These geotextiles are designated as NW10, NW16, and NW24 and had values of mass per unit area equal to 335, 540, and 810 g/m^2, respectively. Material properties for the geotextiles are given in Table 2. The overlying coarse drainage layer consisted of hard angular gravel (crushed rock), with particle sizes ranging from 25 to 38 mm. The soil subgrade consisted of compacted clay or compacted clean angular sand (S). The clay soil was taken from a borrow source for CCL construction at a currently operating municipal solid waste landfill in southern California and is described as Soil #2 in the companion paper (Fox et al. 2014). This material had a liquid limit of 56 and plastic limit of 29, and was passed through a 4.75-mm sieve to remove the gravel fraction. The optimum moisture content (OMC) and maximum dry unit weight were 23.0% and 14.9 kN/m^3, as measured by the standard Proctor test. Fig. 1 presents particle size distributions for the drainage layer, sand subgrade, and clay subgrade, and Fig. 2 shows a photograph of typical gravel particles for the drainage layer.

Table 1. Material Properties for HDPE Geomembrane

Properties	Value
Average/minimum thickness	1.55/1.47 mm
Density	0.949 g/cc
Tensile strength at yield/break	28.4/28.5 kN/m
Tensile elongation at yield/break	18/474%
Tear resistance	231 N
Puncture resistance	636 N
Asperity height	0.61/0.58 mm

Procedures

Geomembrane damage effects were evaluated for multiinterface specimens using the large direct shear machine described by Fox et al. (2006). Specimens were sheared between a rigid pullout plate and the floor of the test chamber, each of which was covered with a rough gripping surface. The shearing area for each specimen was 152 × 1,067 mm. Specimens had three configurations, DL/GT/GM/CCL, DL/GM/S, and DL/GT/GM/S, as shown in Fig. 3. From top to bottom, the DL/GT/GM/CCL specimens consisted of a drainage layer, nonwoven geotextile, geomembrane, and CCL. Using a large hand tamper, CCL subgrades were compacted in two lifts to a final thickness of 50 mm and target water content of 24% (i.e., wet of OMC). The top surface of each CCL was smooth after compaction and was sprayed with 100 mL of water. The geomembrane and geotextile were placed on the CCL, and a 75-mm-thick gravel drainage layer was placed on the geotextile without compaction. The gravel was laterally confined within a metal frame that was completely carried by the gravel layer and could displace as needed without contacting the underlying geomembrane or side walls of the test chamber. The edges of the geomembrane were not fixed or clamped to the shearing surfaces to avoid possible progressive failure effects during shear (Fox and Kim 2008). The pullout plate was then placed on the drainage layer and normal stress was applied to the specimen. Specimens for the DL/GM/S tests consisted of drainage layer, geomembrane, and dry sand. The sand subgrade was compacted using the tamper to a final thickness of 50 mm and had a smooth top surface. Specimens for the DL/GT/GM/S tests were prepared identically to those for the DL/GM/S tests, except that a nonwoven geotextile was placed between the drainage layer and geomembrane. All specimens were tested in the as-prepared condition with no additional water added.

Ten tests were conducted for the experimental program, each consisting of a static pressure stage and a shearing stage. For the static pressure stage, the normal stress was released after 24 h, the position of the geomembrane on top of the subgrade was marked, and the geomembrane was removed and assessed for damage. For the shearing stage, the geomembrane was repositioned to its original location on the subgrade, the specimen was reassembled, and the same normal stress

Table 2. Material Properties for Nonwoven Geotextiles

Geotextile	Mass per unit area (g/m^2)	Grab tensile strength (N)	Grab elongation (%)	Puncture strength (N)	Trapezoidal tear strength (N)
NW10	335	1,155	50	725	445
NW16	540	1,735	50	1,055	665
NW24	810	2,200	50	1,100	880

Note: Manufacturer's minimum average roll values.

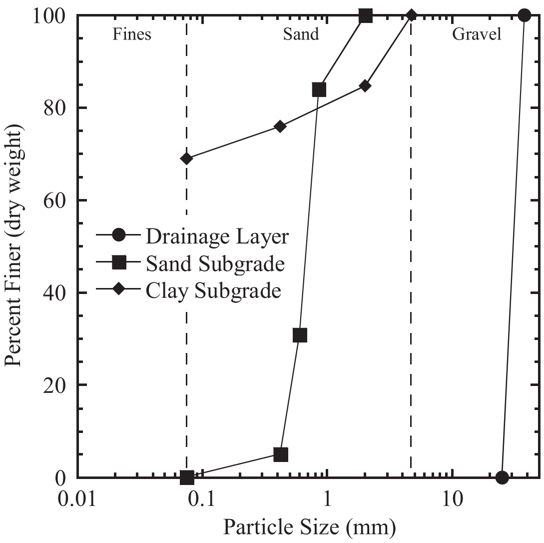

Fig. 1. Particle size distribution curves

Fig. 2. Gravel particles for drainage layer (scale length = 152.4 mm)

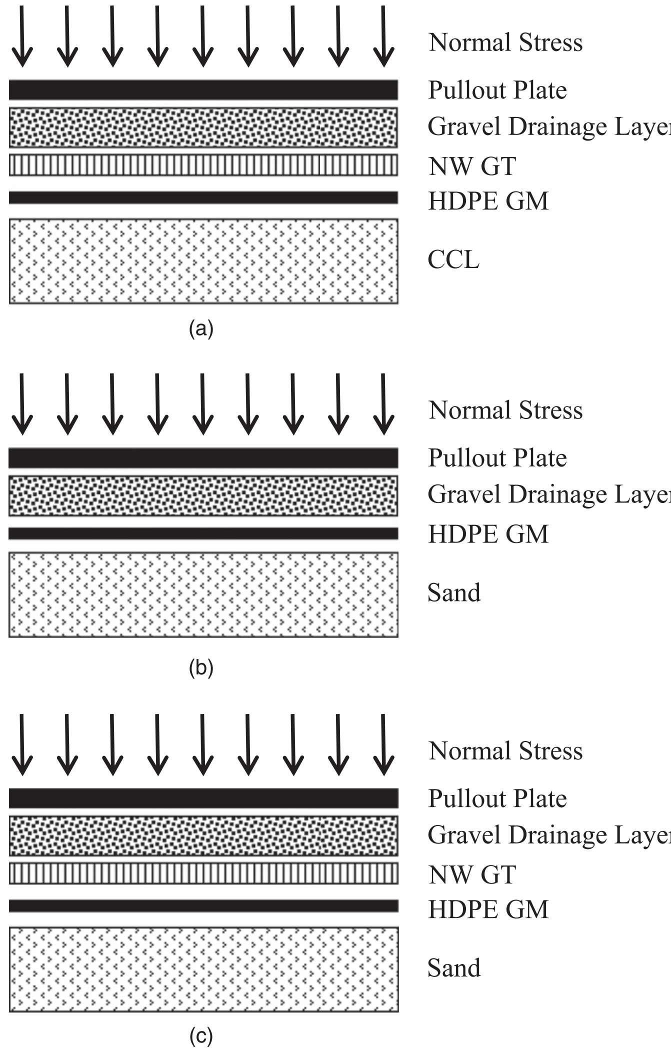

Fig. 3. Specimen configurations for (a) DL/GT/GM/CCL tests; (b) DL/GM/S tests; (c) DL/GT/GM/S tests

was applied for an additional 24 h. The multiinterface specimen was then sheared to a final displacement of 200 mm at a constant displacement rate of 1.0 mm/min. After shearing was completed, the geomembrane was removed and again assessed for damage.

Damage assessments for the geomembrane specimens included visual inspection, a bright light test, and measurement of the number and size of holes. Visual inspections and photographs focused on damage features, such as indentations, scratches, gouges, wrinkles, and holes. For the bright light test, the geomembrane was held against a bright halogen lamp in a dark room. The holes were counted, and the longest and perpendicular (to longest) dimensions of each were measured using a caliper. Hole size was taken as the average of these two measurements. Geotextile specimens were also inspected and similarly assessed for damage after each stage of testing.

Table 3 summarizes the experimental program. Tests P1 and P2 were conducted for a normal stress (σ_n) equal to 345 and 700 kPa using a CCL subgrade and NW16 geotextile. Tests P3 and P7 were conducted for $\sigma_n = 700$ and 1,389 kPa using a sand subgrade and no geotextile. Tests P4–P6 and P8–P10 were conducted as replicates of P3 and P7, respectively, with the NW10, NW16, and NW24 geotextiles used for geomembrane protection.

Table 3. Summary of Experimental Program and Results

Test	Specimen	Normal stress σ_n (kPa)	GT mass per unit area (g/m^2)	Failure interface	Peak shear strength τ_p (kPa)	Large displacement shear strength τ_{200} (kPa)	GT hole count	GT maximum/ average hole size (mm)	GM hole count	GM maximum/ average hole size (mm)
P1	DL/GT/GM/CCL	354	540	GT/GM	143	88	0	—	0	—
P2	DL/GT/GM/CCL	700	540	GT/GM	287	210	0	—	0	—
P3	DL/GM/S	700	0	GM/S	368	368	—	—	0	—
P4	DL/GT/GM/S	700	335	GT/GM	313	250	0	—	1	0.1/0.1
P5	DL/GT/GM/S	700	540	GT/GM	276	193	0	—	0	—
P6	DL/GT/GM/S	700	810	GT/GM	282	157	0	—	0	—
P7	DL/GM/S	1,389	0	GM/S	742	727	—	—	2	9.5/9.1
P8	DL/GT/GM/S	1,389	335	GT/GM	610	595	4	38.2/14.1	5	29.0/17.8
P9	DL/GT/GM/S	1,389	540	GT/GM	514	397	0	—	0	—
P10	DL/GT/GM/S	1,389	810	GT/GM	547	423	0	—	0	—

(a) (b)

Fig. 4. Geomembrane for DL/GT/GM/CCL Test P1 after (a) static pressure stage and (b) shearing stage

Results

Clay Subgrade Tests

Table 3 provides a summary of the experimental results. The first two tests were conducted using a CCL subgrade. Fig. 4 shows Geomembrane P1 after the static pressure stage and after the shearing stage. This test was conducted using protection Geotextile NW16 and a normal stress of 354 kPa. Inspection after the initial 24-h static pressure stage indicated minimal indentations (dimples) resulting from stress concentrations associated with gravel particles in the overlying drainage layer. Failure occurred at the GT/GM interface during the shearing stage. After shearing, Geomembrane P1 displayed some slight longitudinal scratches and shallow indentations but again no significant damage. Bright light tests indicated that no holes were created in the geotextile or geomembrane for this test.

Geomembrane Specimen P2 was tested at $\sigma_n = 700$ kPa using the same geotextile. Fig. 5 shows generally higher levels of geomembrane damage and similar trends at this normal stress level. Prior to shearing, indentations for Geomembrane P2 were more distinct than for Geomembrane P1. After shearing, this geomembrane displayed low levels of damage consisting of wrinkles and indentations. A third test, not included in Table 3, was conducted at $\sigma_n = 1{,}389$ kPa using a CCL subgrade; however, failure occurred within the clay and not at either geomembrane interface. As such, a decision was made to switch to compacted sand subgrades for the remainder of the testing program.

Sand Subgrade Tests

Moderate Normal Stress

Tests P3–P6 were conducted using a subgrade of compacted sand and normal stress of 700 kPa. Figs. 6–9 compare photographs of the geomembrane specimens after static pressure and after interface shear. Fig. 6 shows the condition of Geomembrane P3, which had no protection geotextile. At the end of the static pressure stage, the geomembrane shows minor indentations from the overlying gravel particles. During the subsequent shearing stage, failure occurred underneath the geomembrane just below the GM/S interface. Interface shear produced much more significant deformations in the geomembrane than static pressure alone; however, the bright light

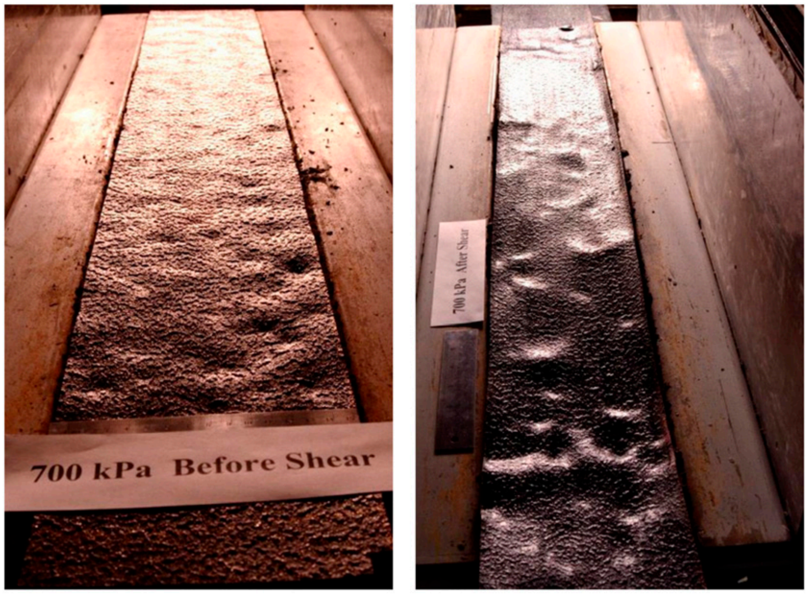

(a) (b)

Fig. 5. Geomembrane for DL/GT/GM/CCL Test P2 after (a) static pressure stage and (b) shearing stage

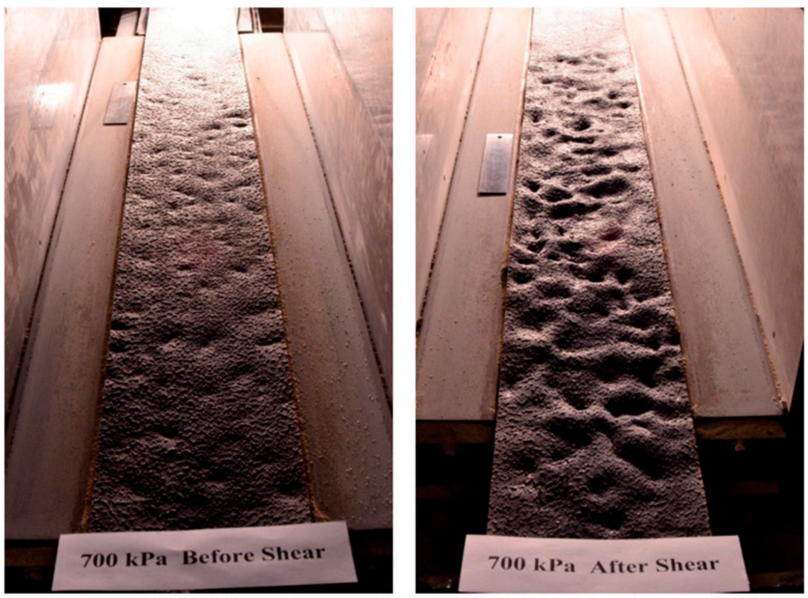

(a) (b)

Fig. 6. Geomembrane for DL/GM/S Test P3 after (a) static pressure stage and (b) shearing stage

test revealed that no holes were created in the geomembrane or geotextile for this test. Fig. 7 compares photographs for geomembrane Specimen P4, which was covered with a lightweight protection geotextile (NW10). Although lower levels of deformation were observed after both static pressure and interface shear as compared with Test P3, the level of geomembrane damage was actually higher. In this case, failure occurred at the GT/GM interface, and the resulting shear of the gravel and geotextile over the geomembrane produced one small hole in the geomembrane (Table 3). Fig. 7 also shows that Geomembrane P4 had significant damage in the form of indentations and wrinkles after the shearing stage.

The use of medium-weight (NW16) and heavyweight (NW24) geotextiles for Tests P5 and P6 resulted in progressively less geomembrane damage, as shown in Figs. 8 and 9. Although no holes were created in either geomembrane specimen, shear displacement again produced more damage than static pressure alone. A comparison of Figs. 5 and 8 also provides information regarding the effect of soil subgrade type on geomembrane damage. Tests P2 and P5 were performed for the same conditions and experienced the same GM/GT interface failure mode. The photographs indicate that the sand subgrade produced similar, but slightly lower, levels of geomembrane damage than the clay subgrade after each stage of testing.

High Normal Stress

Tests P7–P10 were conducted as replicates of Tests P3–P6, except that the normal stress was increased to $\sigma_n = 1{,}389$ kPa. Fig. 10 compares

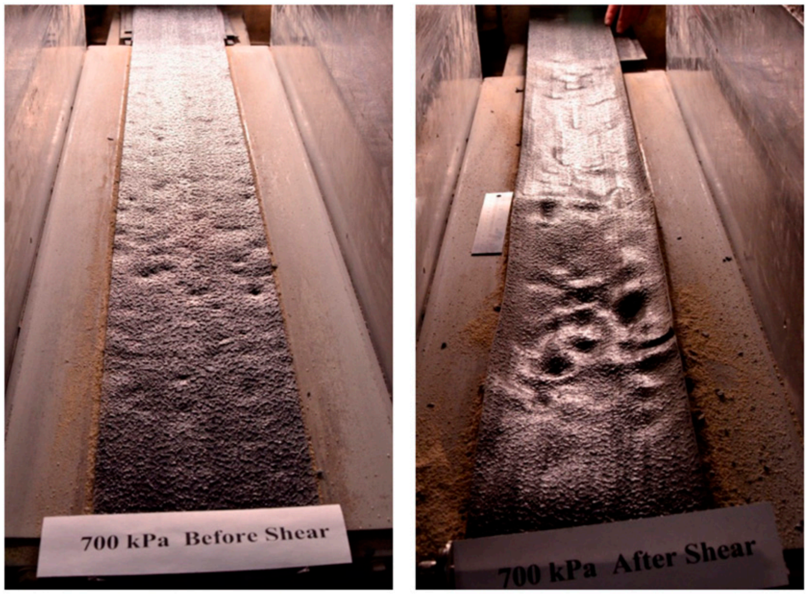

(a) (b)

Fig. 7. Geomembrane for DL/GT/GM/S Test P4 after (a) static pressure stage and (b) shearing stage

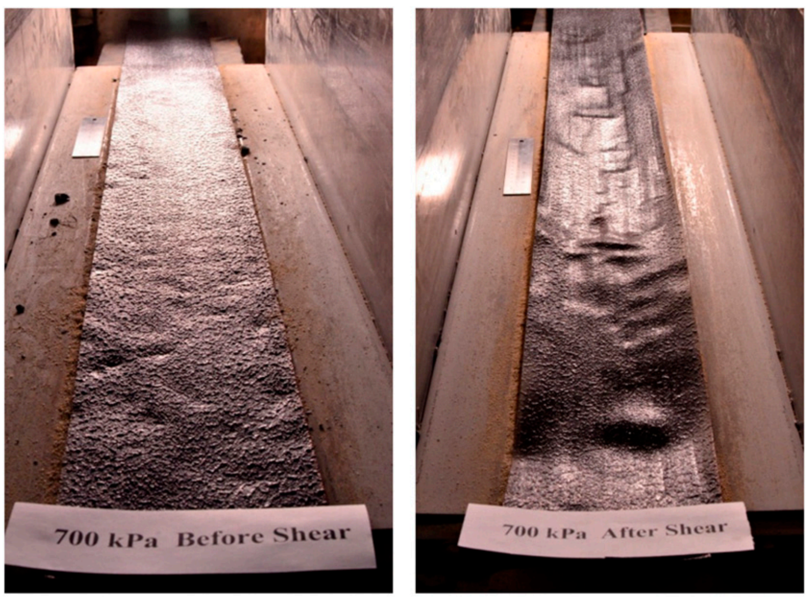

(a) (b)

Fig. 8. Geomembrane for DL/GT/GM/S Test P5 after (a) static pressure stage and (b) shearing stage

photographs of Geomembrane P7, with no protection geotextile, after the static pressure stage and after the shearing stage. Fig. 11 shows a close-up view of the final condition. Prior to shear, this specimen showed minor indentations due to stress concentrations from the overlying gravel layer. After shear to 200 mm, the level of damage increased significantly. Similar to Test P3, failure occurred just below the GM/S interface. However, in this case, interface shear under the higher normal stress created two holes in the geomembrane, with a maximum size of 9.5 mm. In addition, geomembrane deformation in the form of indentations and wrinkles was significantly greater.

Geomembrane P8 was protected by the lightweight geotextile (NW10) and experienced the highest levels of damage observed for the experimental program. Photographs of the geomembrane, geotextile, and sand subgrade are presented in Figs. 12–14. Prior to shear, this geomembrane showed minor indentations. Similar to Test P4, shear failure occurred at the GT/GM interface and produced significantly higher levels of damage (Fig. 12). Interface shear created five holes in the geomembrane, with a maximum size of 29.0 mm. The hole count for this specimen translates to an average of 31 holes/m^2. Inspection of the geotextile after the shearing stage revealed four holes with a maximum size of 38.2 mm. Fig. 13 shows close-up views of the largest holes. The observed levels of wrinkling, gouging, and puncture damage to Geomembrane P8 as a result of interface shear are considered to be severe.

The level of damage for Geomembranes P4 and P8, which had lightweight geotextiles for protection, was higher than the damage

(a) (b)

Fig. 9. Geomembrane for DL/GT/GM/S Test P6 after (a) static pressure stage and (b) shearing stage

(a) (b)

Fig. 10. Geomembrane for DL/GM/S Test P7 after (a) static pressure stage and (b) shearing stage

for Geomembranes P3 and P7, which had no protection geotextiles. This surprising result occurred because the location of the failure surface was controlled by the geotextiles. Direct sliding of the gravel and geotextile over the geomembranes produced more holes than sliding of the geomembranes over the sand subgrade. Thus, depending on conditions, the use of a lightweight geotextile may actually provide less protection to a geomembrane than no geotextile at all. This illustrates the general importance of conducting project-specific shear tests, including multiinterface tests, to assess possible geomembrane damage and determine failure modes and corresponding shear strengths for the design of liner systems.

Figs. 15 and 16 show Geomembranes P9 and P10, which were tested using the medium-weight (NW16) and heavyweight (NW24) geotextiles, respectively. Similar to Tests P5 and P6, interface shear caused significantly more geomembrane damage than static pressure alone, and the amount of shear-induced damage decreased with increasing geotextile mass/area. Although no holes were created in either geomembrane, the amount of damage is significant. A close-up view of Geomembrane P10, shown in Fig. 17, indicates that substantial wrinkle damage occurred even when using the heavyweight geotextile at this normal stress level.

Stress-Displacement Relationships

Fig. 18 compares the shear stress τ versus shear displacement Δ relationships measured during the shearing stage for all 10 tests.

Table 3 lists peak τ_p and large displacement τ_{200} shear strengths. Each relationship shows a generally familiar response consisting of a rapid rise to peak strength followed by a gradual transition to constant or near-constant strength at large displacements. For consistent conditions, shear strength increases with increasing normal stress, as expected. Close inspection of these relationships, however, reveals more interesting trends.

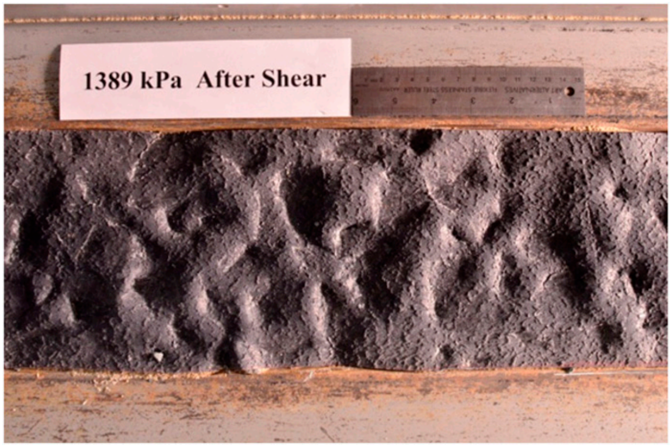

Fig. 11. Geomembrane for DL/GM/S Test P7 after shearing stage

First, the clay subgrade relationships display a less stiff (i.e., lower modulus) response leading to peak strength than the sand subgrade relationships, as might be expected. Second, Test P2 with a clay subgrade yields a slightly higher shear strength than Test P5 with a sand subgrade, which was conducted for the same conditions. This is consistent with the slightly higher indentation damage observed for Geomembrane P2. Third, all tests with GT/GM interface failures show postpeak strength reduction, which occurs primarily due to abrasion of the geomembrane texturing (Li and Gilbert 2006). However, the two tests that failed below the geomembrane (P3 and P7) experienced no postpeak reduction. This is curious considering that a geomembrane sheared over sand would normally be expected to experience postpeak strength reduction as well (Dove and Frost 1999; Fleming et al. 2006). However, rather than being attached to a hard backing plate, these geomembranes were placed within multiinterface specimens and experienced out-of-plane deformation under the gravel contacts (e.g., Fig. 11). As a result, failure actually occurred within the sand layer just below the undulations of the GM/S interface, and the likely contractive response of the sand under the high normal stress yielded a stress-displacement relationship with no postpeak reduction. Fourth, Fig. 18 indicates that shear strength for the sand subgrade tests at each normal stress level correlates with mass/area of the protection geotextile. Peak and large displacement

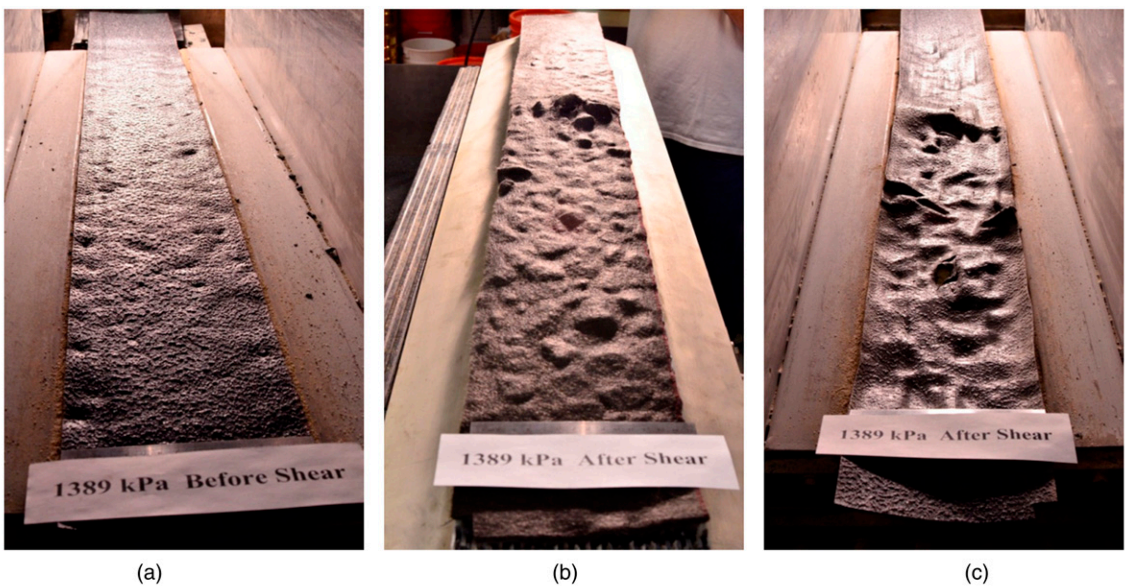

Fig. 12. Specimens for DL/GT/GM/S Test P8: (a) geomembrane after static pressure stage; (b) nonwoven geotextile after shearing stage; (c) geomembrane after shearing stage

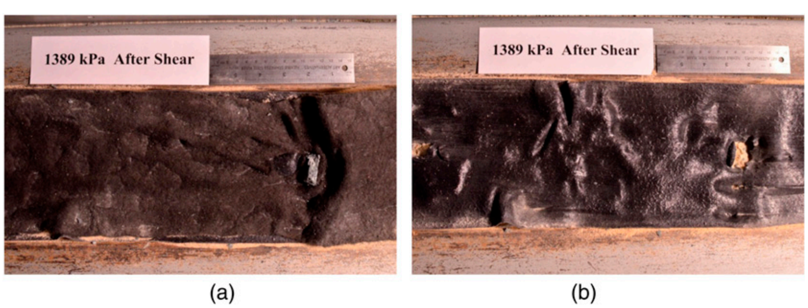

Fig. 13. Specimens for DL/GT/GM/S Test P8: (a) nonwoven geotextile after shearing stage; (b) geomembrane after shearing stage

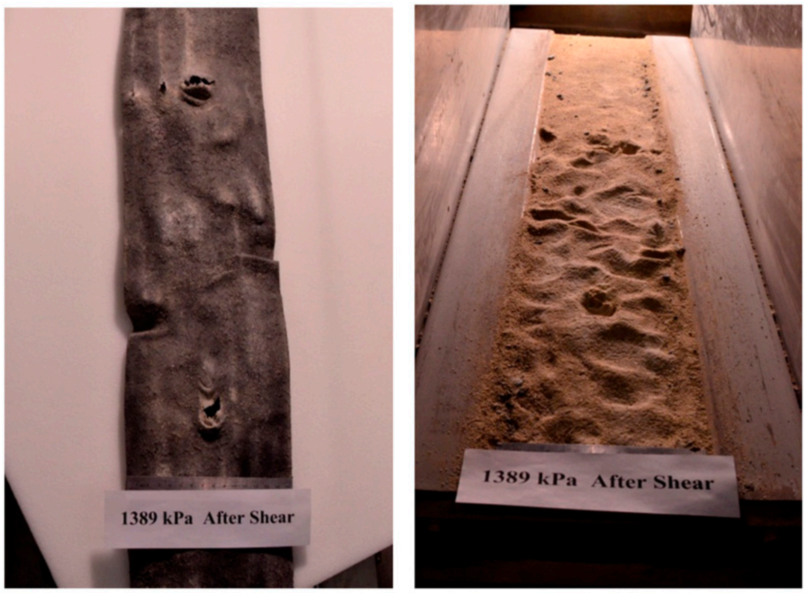

(a) (b)

Fig. 14. Specimens for DL/GT/GM/S Test P8: (a) geomembrane (bottom side) after shearing stage; (b) sand subgrade after shearing stage

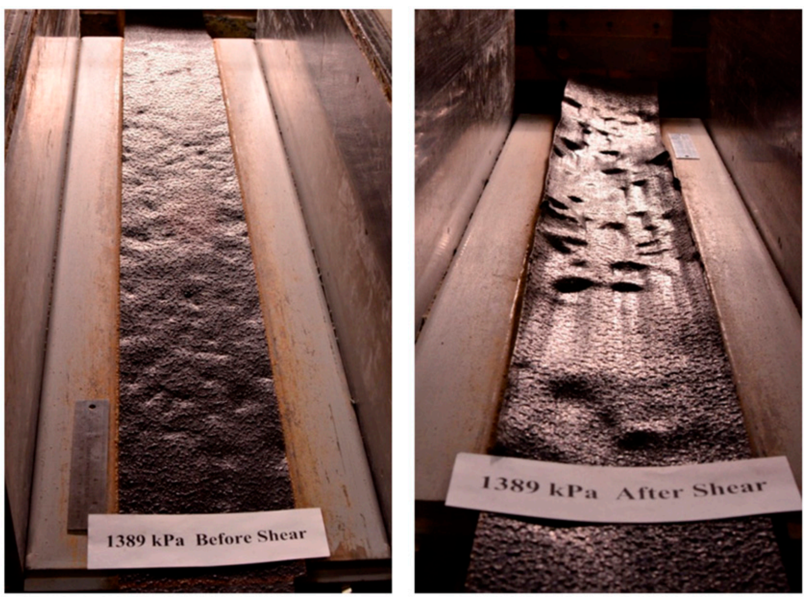

(a) (b)

Fig. 15. Geomembrane for DL/GT/GM/S Test P9 after (a) static pressure stage and (b) shearing stage

strengths were highest with no protection geotextile (P3 and P7) and then generally decreased with increasing geotextile mass/area. Similar to the findings of Breitenbach and Swan (1999), interface shear strength increased due to greater magnitudes of geomembrane out-of-plane deformation and associated interlocking with adjacent materials. Fig. 18 indicates that this effect can be important. For example, the large displacement shear strength for Test P4 is 59% higher than for Test P6 even though both were sheared at σ_n = 700 kPa and experienced the same failure mode. Although beneficial in terms of shear strength, greater interlocking between a gravel layer and an underlying geomembrane can be highly detrimental to the integrity of the geomembrane. Finally, considering the findings of the companion paper (Fox et al. 2014), irregularity of the postpeak response for Test P7 and the gradually increasing large displacement strength for Test P8 may reflect increasing levels of geomembrane damage during the course of shear displacement.

Implications for Practice and Research

Engineering Design

Results from the preceding experimental investigation of shear-induced damage to a HDPE geomembrane beneath a gravel drainage

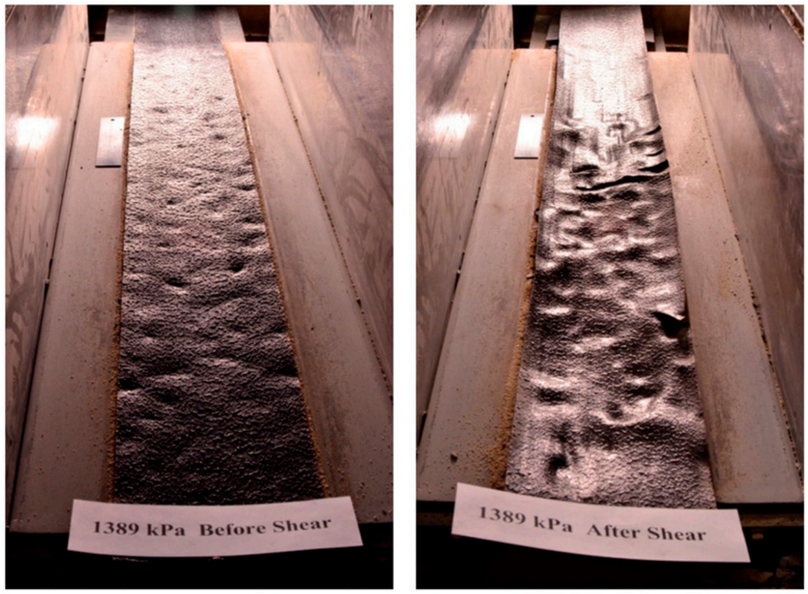

(a) (b)

Fig. 16. Geomembrane for DL/GT/GM/S Test P10 after (a) static pressure stage and (b) shearing stage

Fig. 17. Geomembrane for DL/GT/GM/S Test P10 after shearing stage

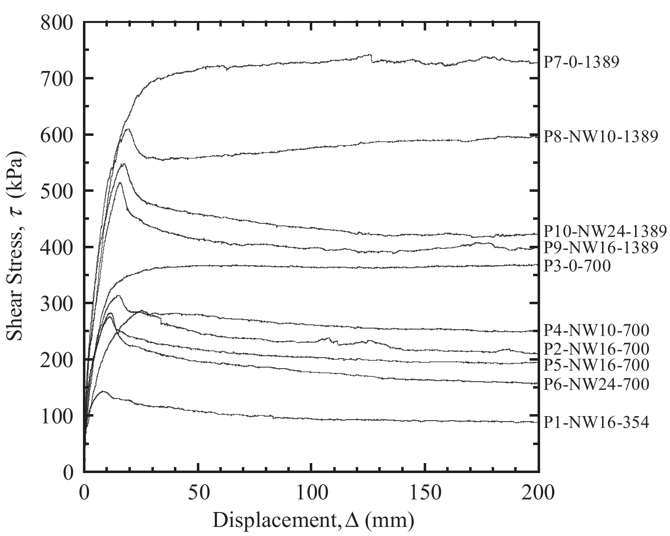

Fig. 18. Shear stress-displacement relationships

layer, with and without a protection nonwoven geotextile, have potentially important implications for the design of facilities that use these materials for bottom liner systems. Large-scale direct shear tests have indicated that shear displacement of a gravel layer and nonwoven geotextile over a geomembrane under moderate to high normal stress conditions can cause much greater damage to the geomembrane than static pressure alone. Depending on conditions, severe damage is possible, such as the measured average of 31 holes/m^2 for Geomembrane P8. This finding is especially significant considering that all of the geomembranes in this study experienced, at most, minor damage under static pressure. Moreover, NW GT/GM interfaces are often critical for stability and may experience large local shear displacements on side slopes from waste settlement, even if the global factor of safety is adequate (Jones and Dixon 2005; Sia and Dixon 2012). Shear displacements can also occur on base liners from seismic loading and buttressing of waste fills (Filz et al. 2001; Zania et al. 2010; Kavazanjian et al. 2011). The extensive body of past research on geomembrane protection has not accounted for possible additional damage caused by static pressure combined with interface shear. Thus, currently accepted standards of practice for the protection of geomembranes from overlying gravel drainage layers in bottom liner systems, at least those involving nonwoven geotextiles, may lead to unanticipated vulnerability for these geomembranes. In general, the test results suggest that heavier nonwoven geotextiles may be needed in U.S. practice to provide adequate geomembrane protection from overlying coarse gravel drainage layers when interface shear is expected under moderate to high normal stress conditions.

Direct Shear Testing

The experimental results also have important implications for direct shear testing practice. The primary reason that shear-induced geomembrane damage from overlying coarse soil layers has not been previously reported is probably because current practice typically calls for single-interface shear tests. For the current investigation, this would require testing the nonwoven geotextile against the geomembrane and then separately testing the drainage layer against the nonwoven geotextile. Multiinterface tests are generally not performed, and important material interactions, such as those investigated in the current study, are not evaluated. Based on these considerations, direct shear tests should be conducted using multiinterface specimens and project-specific conditions. Thus, a geomembrane should be placed between actual field materials, not clamped to a hard backing plate, and sheared for normal stress conditions expected in the field. The appropriate stress range for deep landfills and heap leach pads may require the use of specialized high-capacity equipment. Development or revision of standard test procedures may be necessary to account for multiinterface specimens and assessment of possible geomembrane damage due to interface shear.

Future Research Needs

Limitations of the current study highlight the need for future research. Additional investigations are needed to better understand the effects of gravel particle characteristics (e.g., size, angularity, and hardness), normal stress level, subgrade soil type, and magnitude of shear displacement on shear-induced geomembrane damage. In particular, the risk posed by borderline materials, such as drainage layers containing smaller, less angular gravel, requires investigation. Detailed quantitative studies of geomembrane deformation would be useful for borderline cases. Research is also needed to evaluate other protection materials and the effects of geomembrane polymer type, thickness, and temperature. Finally, the general applicability of the static pressure performance test for assessment of geomembrane damage may need to be reevaluated for field conditions that involve possible interface shear displacement. Development of new standard test procedures may be warranted and reconsideration of geomembrane protection guidelines may be necessary in light of new data that include the effects of such displacement.

Conclusions and Recommendations

The following conclusions are based on the foregoing experimental investigation of shear-induced damage to a HDPE geomembrane under a gravel drainage layer, with and without a nonwoven geotextile protection layer at the interface:

1. Geomembrane specimens subjected to 24 h of static pressure (i.e., no shear) displayed, at most, minor damage in the form of indentations under the gravel contacts. Geomembrane damage increased with increasing normal stress and decreasing mass/area of the nonwoven geotextile. No holes were created in the geomembranes for any of the static pressure tests.
2. Shear displacement of a gravel drainage layer and nonwoven geotextile over a geomembrane under moderate to high normal stress conditions can cause much greater damage to the geomembrane than static pressure alone. The greatest damage occurred at the highest normal stress level (1,389 kPa) using a lightweight geotextile ($335\ g/m^2$) and yielded an average of $31\ holes/m^2$, with a maximum hole size of 29 mm. Significant geomembrane damage was observed at the highest normal stress level even when using a heavyweight ($810\ g/m^2$) geotextile.
3. Shear-induced geomembrane damage increased with increasing normal stress and decreasing mass/area of the nonwoven geotextile. Geomembrane damage measured using a lightweight protection geotextile was greater than damage measured using no protection geotextile due to a change in failure surface location.
4. For the same conditions, a compacted sand subgrade produced similar, but slightly lower, levels of geomembrane damage than a compacted clay subgrade.
5. Shear strength of the multiinterface specimens increased significantly with decreasing mass/area of the nonwoven geotextile, which likely occurred due to greater out-of-plane deformation and associated interlocking of the geomembrane with adjacent materials. Although beneficial in terms of shear strength, greater interlocking between a gravel layer and an underlying geomembrane can be highly detrimental to the integrity of the geomembrane.
6. The experimental results illustrate the general importance of conducting project-specific shear tests, including multiinterface tests, to assess possible geomembrane damage and determine failure modes and corresponding shear strengths for the design of liner systems.

Subject to further assessment and verification, the following provisional recommendations can be made at this time. The placement of a gravel drainage layer on top of a HDPE geomembrane with a protection nonwoven geotextile can be considered for landfill cover systems and other low-stress applications, but should be viewed with caution for landfill bottom liner systems and other moderate- to high-stress applications. If a gravel drainage layer is considered for a bottom liner and there is a reasonable expectation for interface shear displacement with a geomembrane, project-specific direct shear tests should be conducted to determine the potential for shear-induced geomembrane damage. Recommendations are provided for the performance of such tests. If these tests indicate significant damage, a designer has several options: (1) reduce the size and/or angularity of gravel particles; (2) increase the mass/area of the nonwoven geotextile; (3) switch to a different type of protection layer; or (4) include an intentional slip surface above the liner to limit shear displacement at the geomembrane interface. Options 1–3 are preferred because Option 4 can be difficult to implement and will not protect the geomembrane from static pressure damage. In general, the test results suggest that heavier nonwoven geotextiles may be needed in U.S. practice to provide adequate geomembrane protection from overlying coarse drainage layers when interface shear is expected under moderate to high normal stress conditions.

Acknowledgments

Financial support for this investigation was provided by Grant No. CMMI-0800030 from the Geotechnical Engineering Program of the U.S. National Science Foundation. Geomembrane materials were provided by PolyFlex, and geotextile materials were provided by GSE. Clay soil was obtained through the assistance of Dr. Neven Matasovic of Geosyntec Consultants, Huntington Beach, California. This support and assistance is gratefully acknowledged. The authors also thank Neven for helpful information with regard to the current state of landfill design practice for geomembrane protection under gravel drainage layers.

References

Brachman, R. W. I., and Sabir, A. (2013). "Long-term assessment of a layered-geotextile protection layer for geomembranes." *J. Geotech. Geoenviron. Eng.*, 10.1061/(ASCE)GT.1943-5606.0000812, 752–764.

Breitenbach, A. J., and Swan, R. H., Jr. (1999). "Influence of high load deformations on geomembrane liner interface strengths." *Proc., Geosynthetics '99*, Vol. 1, Industrial Fabrics Association Int., Roseville, MN, 517–529.

Christie, M. A., and Smith, M. E. (2013). "A brief history of heap leaching." *Proc., GRI-25*, Industrial Fabrics Association Int., Roseville, MN, 265–287.

Dickinson, S., and Brachman, R. W. I. (2008). "Assessment of alternative protection layers for a geomembrane–geosynthetic clay liner (GM–GCL) composite liner." *Can. Geotech. J.*, 45(11), 1594–1610.

Dixon, N., Zamara, K., Jones, D. R. V., and Fowmes, G. (2012). "Waste/lining system interaction: Implications for landfill design and performance." *Geotech. Eng. J. SEAGS AGSSEA*, 43(3), 1–10.

Dove, J. E., and Frost, J. D. (1999). "Peak friction behavior of smooth geomembrane-particle interfaces." *J. Geotech. Geoenviron. Eng.*, 10.1061/(ASCE)1090-0241(1999)125:7(544), 544–555.

Filz, G. M., Esterhuizen, J. J. B., and Duncan, J. M. (2001). "Progressive failure of lined waste impoundments." *J. Geotech. Geoenviron. Eng.*, 10.1061/(ASCE)1090-0241(2001)127:10(841), 841–848.

Fleming, I. R., and Rowe, R. K. (2004). "Laboratory studies of clogging of landfill leachate collection and drainage systems." *Can. Geotech. J.*, 41(1), 134–153.

Fleming, I. R., Sharma, J. S., and Jogi, M. B. (2006). "Shear strength of geomembrane-soil interface under unsaturated conditions." *Geotext. Geomembr.*, 24(5), 274–284.

Fox, P. J., and Kim, R. H. (2008). "Effect of progressive failure on measured shear strength of geomembrane/GCL interface." *J. Geotech. Geoenviron. Eng.*, 10.1061/(ASCE)1090-0241(2008)134:4(459), 459–469.

Fox, P. J., Nye, C. J., Morrison, T. C., Hunter, J. G., and Olsta, J. T. (2006). "Large dynamic direct shear machine for geosynthetic clay liners." *J. ASTM Geotech. Test.*, 29(5), 392–400.

Fox, P. J., Ross, J. D., Sura, J. M., and Thiel, R. S. (2011). "Geomembrane damage due to static and cyclic shearing over compacted gravelly sand." *Geosynthetics Int.*, 18(5), 272–279.

Fox, P. J., and Thielmann, S. S. (2014). "Damage to HDPE geomembrane from interface shear with gravel drainage layer and protection layer." *J. Geotech. Geoenviron. Eng.*, 10.1061/(ASCE)GT.1943-5606.0001063, 02813001.

Fox, P. J., Thielmann, S. S., Stern, A. N., and Athanassopoulos, C. (2014). "Interface shear damage to a HDPE geomembrane. I: Gravelly compacted clay liner." *J. Geotech. Geoenviron. Eng.*, 10.1061/(ASCE)GT.1943-5606.0001132, 04014039.

Giroud, J. P. (1973). "L'étancheité des retenues d'eau par feuilles déroulées." *Annales de l'ITBTP*, 312, TP 161, 96–112 (in French).

Giroud, J. P. (1982). "Design of geotextiles associated with geomembranes." *Proc., 2nd Int. Conf. on Geotextiles*, Vol. 1, Industrial Fabrics Association Int., Roseville, MN, 37–42.

Giroud, J. P., and Touze-Foltz, N. (2003). "Geomembranes in landfills: Discussion at the 7th International Conference on Geosynthetics." *Geosynthetics Int.*, 10(4), 124–133.

Heerten, G. (1994). "Geotextile and/or GCL protection systems for geomembranes." *Geosynthetic liner systems: Innovations, concerns and designs,* R. M. Koerner and R. F. Wilson-Fahmy, eds., Industrial Fabrics Association Int., Roseville, MN, 155–167.

Hornsey, W. P., and Wishaw, D. M. (2012). "Development of a methodology for the evaluation of geomembrane strain and relative performance of cushion geotextiles." *Geotext. Geomembr.*, 35, 87–99.

Hullings, D. E., and Koerner, R. M. (1991). "Puncture resistance of geomembranes using a truncated cone test." *Proc., Geosynthetics '91*, Vol. 1, Industrial Fabrics Association Int., Roseville, MN, 273–285.

Jones, D. R. V., and Dixon, N. (2005). "Landfill lining stability and integrity: The role of waste settlement." *Geotext. Geomembr.*, 23(1), 27–53.

Kavazanjian, E., Jr., Arab, G. M., and Matasovic, N. (2011). "Seismic analysis of heap leach pad liner systems." *Proc., 5th Int. Conf. on Earthquake Geotechnical Engineering* (CD-ROM), Chilean Geotechnical Society, Santiago, Chile.

Koerner, R. M., Hsuan, Y. G., Koerner, G. R., and Gryger, D. (2010). "Ten year creep puncture study of HDPE geomembranes protected by needle-punched nonwoven geotextiles." *Geotext. Geomembr.*, 28(6), 503–513.

Li, M.-H., and Gilbert, R. B. (2006). "Mechanism of post-peak strength reduction for textured geomembrane-nonwoven geotextile interfaces." *Geosynthetics Int.*, 13(5), 206–209.

McIsaac, R., and Rowe, R. K. (2007). "Clogging of gravel drainage layers permeated with landfill leachate." *J. Geotech. Geoenviron. Eng.*, 10.1061/(ASCE)1090-0241(2007)133:8(1026), 1026–1039.

Motan, E. S., Reed, L. S., and Lundell, C. M. (1993). "Geomembrane protection by nonwoven geotextiles." *Proc., Geosynthetics '93*, Vol. 2, Industrial Fabrics Association Int., Roseville, MN, 887–900.

Narejo, D., Koerner, R. M., and Wilson-Fahmy, R. F. (1996). "Puncture protection of geomembranes. Part II: Experimental." *Geosynthetics Int.*, 3(5), 629–653.

Nosko, V., and Touze-Foltz, N. (2000). "Geomembrane liner failure: Modeling of its influence on contaminant transfer." *Proc., 2nd European Conf. on Geosynthetics*, A. Cancelli, D. Cazzuffi, and C. Soccodato, eds., Pàtron Editore, Bologna, Italy, 557–560.

Peggs, I. D., Schmucker, B., and Carey, P. (2005). "Assessment of maximum allowable strains in polyethylene and polypropylene geomembranes." *Proc., GeoFrontiers 2005: Waste Containment and Remediation*, A. Alshawabkeh, et al., eds., ASCE, Reston, VA, 1–16.

Reddy, K. R., Bandi, S. R., Rohr, J. J., Finy, M., and Siebken, J. (1996a). "Field evaluation of protective covers for landfill geomembrane liners under construction loading." *Geosynthetics Int.*, 3(6), 679–700.

Reddy, K. R., Kosgi, S., and Motan, E. S. (1996b). "Interface shear behavior of landfill composite liner systems: A finite element analysis." *Geosynthetics Int.*, 3(2), 247–275.

Rowe, R. K., Armstrong, M. D., and Cullimore, D. R. (2000). "Particle size and clogging of granular media permeated with leachate." *J. Geotech. Geoenviron. Eng.*, 10.1061/(ASCE)1090-0241(2000)126:9(775), 775–786.

Rowe, R. K., Quigley, R. M., Brachman, R. W. I., and Booker, J. R. (2004). *Barrier systems for waste disposal facilities*, 2nd Ed., Spon, London.

Sia, A. H. I., and Dixon, N. (2012). "Numerical modeling of landfill lining system—Waste interaction: Implications of parameter variability." *Geosynthetics Int.*, 19(5), 393–408.

Stark, T. D., and Poeppel, A. R. (1994). "Landfill liner interface strengths from torsional-ring-shear tests." *J. Geotech. Engrg.*, 10.1061/(ASCE)0733-9410(1994)120:3(597), 597–615.

Thiel, R., and Smith, M. E. (2003). "State of the practice review of heap leach pad design issues." *Proc., 17th GRI Conf., Hot Topics in Geosynthetics-IV*, Geosynthetics Institute, Folsom, PA.

Tognon, A. R., Rowe, R. K., and Moore, I. D. (2000). "Geomembrane strain observed in large-scale testing of protection layers." *J. Geotech. Geoenviron. Eng.*, 10.1061/(ASCE)1090-0241(2000)126:12(1194), 1194–1208.

Zamara, K. A., Dixon, N., Jones, D. R. V., and Fowmes, G. (2012). "Monitoring of a landfill side slope lining system: Instrument selection, installation and performance." *Geotext. Geomembr.*, 35, 1–13.

Zania, V., Tsompanakis, Y., and Psarropoulos, P. N. (2010). "Seismic displacements of landfills and deformation of geosynthetics due to base sliding." *Geotext. Geomembr.*, 28(6), 491–502.

Zanzinger, H. (1999). "Efficiency of geosynthetic protection layers for geomembrane liners: Performance in a large-scale model test." *Geosynthetics Int.*, 6(4), 303–317.

J. Geotech. Geoenviron. Eng. 2014.140.